Biochimica et Biophysica Acta 1844 (2014) 1193–1200

Contents lists available at ScienceDirect

Biochimica et Biophysica Acta

journal homepage: www.elsevier.com/locate/bbapap

Single tryptophan mutants of FtsZ: Nucleotide binding/exchange and conformational transitions

Felipe Montecinos-Franjola [a,1], Nicholas G. James [b], Luis Concha-Marambio [a,2], Juan E. Brunet [c], Rosalba Lagos [a], Octavio Monasterio [a], David M. Jameson [b,*]

[a] Laboratorio de Biología Estructural y Molecular, Departamento de Biología, Facultad de Ciencias, Universidad de Chile, Santiago 7800024, Chile
[b] Department of Cell and Molecular Biology, John A. Burns School of Medicine, University of Hawaii, Honolulu 96813, HI, USA
[c] Instituto de Química, Facultad de Ciencias, Pontificia Universidad Católica de Valparaíso, Valparaíso 2373223, Chile

ARTICLE INFO

Article history:
Received 7 October 2013
Received in revised form 24 March 2014
Accepted 26 March 2014
Available online 2 April 2014

Keywords:
FtsZ
Conformational change
Equilibrium unfolding
Tryptophan fluorescence
Time-resolved fluorescence
Phasor plot

ABSTRACT

Cell division protein FtsZ cooperatively self-assembles into straight filaments when bound to GTP. A set of conformational changes that are linked to FtsZ GTPase activity are involved in the transition from straight to curved filaments that eventually disassemble. In this work, we characterized the fluorescence of single Trp mutants as a reporter of the predicted conformational changes between the GDP- and GTP-states of *Escherichia coli* FtsZ. Steady-state fluorescence characterization showed the Trp senses different environments and displays low solvent accessibility. Time-resolved fluorescence data indicated that the main conformational changes in FtsZ occur at the interaction surface between the N and C domains, but also minor rearrangements were detected in the bulk of the N domain. Surprisingly, despite its location near the bottom protofilament interface at the C domain, the Trp 275 fluorescence lifetime did not report changes between the GDP and GTP states. The equilibrium unfolding of FtsZ features an intermediate that is stabilized by the nucleotide bound in the N-domain as well as by quaternary protein–protein interactions. In this context, we characterized the unfolding of the Trp mutants using time-resolved fluorescence and phasor plot analysis. A novel picture of the structural transition from the native state in the absence of denaturant, to the solvent-exposed unfolded state is presented. Taken together our results show that conformational changes between the GDP and GTP states of FtsZ, such as those observed in FtsZ unfolding, are restricted to the interaction surface between the N and C domains.

1. Introduction

Cell division protein FtsZ polymerizes at the middle of the cell to form the Z-ring which provides constriction force for initiation of cytokinesis [1]. In vitro, FtsZ bound to GTP self-assembles into straight filaments and magnesium-induced hydrolysis of the nucleotide drives depolymerization [2,3]. Electron microscopy shows that stabilized FtsZ-GDP polymers adopt a helix-like shape that differs from the straight polymers observed in solutions of FtsZ-GTP [4,5]. These findings suggest a different conformation of the monomer depending on the bound nucleotide, acting as switch in the assembly-disassembly process that drives Z-ring constriction. The crystal structure of FtsZ shows two globular domains, the nucleotide binding N domain and the catalytic C domain, that are connected by the central H7 helix [6]. Although many crystals of FtsZ have been reported to date, all were considered to be in the curved form [7,8]. Only recently was a clear change in FtsZ conformation, regarded as the straight form, reported in the crystal structure of *Staphylococcus aureus* FtsZ in complex with the cell-division inhibitor PC190723, [9,10]. Computational analyzes on FtsZ crystals described flexible segments in the FtsZ sequence mainly located in the C domain [11–13]. Martín-Galiano et al. [12] identified FtsZ mutations located between H7 helix and the C domain that presumably blocked the switch from straight to curved conformations. We investigated the disrupting effect of Trp mutations on the FtsZ structure and function (*Escherichia coli* FtsZ lacks Trp residues in its sequence) and found that tyrosine in position 222 is a key residue in FtsZ polymerization (unpublished data and [11]). More recently, Chen and Erickson [14] characterized the same mutation, Y222W, and based on fluorescence quenching experiments, proposed a movement leading to a separation of the N and C domains that followed FtsZ assembly. These accumulated data indicated that the nucleotide-mediated conformational changes

Abbreviations: GDP, GTP, Guanosine diphosphate, triphosphate; Trp, Tryptophan; GdmCl, Guanidinium chloride

* Corresponding author at: 651 Ilalo Street, Biosciences 222, Honolulu, Hawaii 96813, USA. Tel.: +1 808 956 8332.
E-mail addresses: felipe.montecinos@nih.gov (F. Montecinos-Franjola), njames4@hawaii.edu (N.G. James), luis.m.concha@uth.tmc.edu (L. Concha-Marambio), jbrunet@ucv.cl (J.E. Brunet), rolagos@uchile.cl (R. Lagos), monaster@uchile.cl (O. Monasterio), djameson@hawaii.edu (D.M. Jameson).
[1] Present address: Eunice Kennedy Shriver National Institute of Child Health and Human Development (NICHD), Bethesda, MD 20892, USA.
[2] Present address: Department of Neurology, The University of Texas Health Science Center, Houston, TX 77030, USA.

http://dx.doi.org/10.1016/j.bbapap.2014.03.012
1570-9639/

attributed to the transition from straight to curved filaments involve hinge-like movements between N and C domains. In fact, the structure of the FtsZ-PC190723 complex shows a striking new orientation between the otherwise structurally unmodified N and C domains, in accordance with experiments.

In this work, we used time-resolved fluorescence of FtsZ Trp mutants as a reporter of the local conformational transitions related to the nucleotide bound state at equilibrium. A FtsZ structural model is depicted in Fig. 1, where the nucleotide binding domain (N domain) is colored blue, the catalytic domain (C domain) is colored red, and the plane of interaction between both domains is indicated by the H7-helix, colored in cyan. The Trp mutants were selected based on their locations in the FtsZ structure. As seen in the model, the F40W mutation (side chain in orange) is located on the nucleotide binding domain; the Y222W mutation (side chain in green) is located on the interface between both domains, and the F275W mutation (side chain in yellow) is located on the catalytic domain. This study was extended to characterization of the conformational transitions in FtsZ unfolding, which we previously described using the classic a linear extrapolation method [11,15,16]. In the past, we have applied time-resolved fluorescence methods to study protein conformational changes and unfolding [17–19], and more recently, we exploited the phasor method to describe complex fluorescence decays of fluorophore mixtures and of biological samples [20,21]. Here, we describe the application of the phasor plot method to the time-resolved fluorescence of FtsZ Trp mutants.

2. Materials and methods

2.1. Protein purification and additional methods

Details on protein purification, determination of protein concentration and nucleotide content, measurement of secondary structure by CD and measurement of mant-GDP and mant-GTP dissociation constants can be found in the supporting information.

2.2. GTPase activity and polymerization

The GTPase activity and polymerization of FtsZ wt and of the Trp mutants were measured by the malachite green colorimetric assay and by 90° angle light scattering at 350 nm, respectively, as previously described [22]. The reaction mixtures contained FtsZ wt or the Trp mutants at desired protein concentration dissolved in 50 mM Mes-KOH pH 6.5, 50 mM KCl, and 10 mM $MgCl_2$ and were incubated at 30 °C. The polymerization reaction was started by the addition of 0.5 mM GTP.

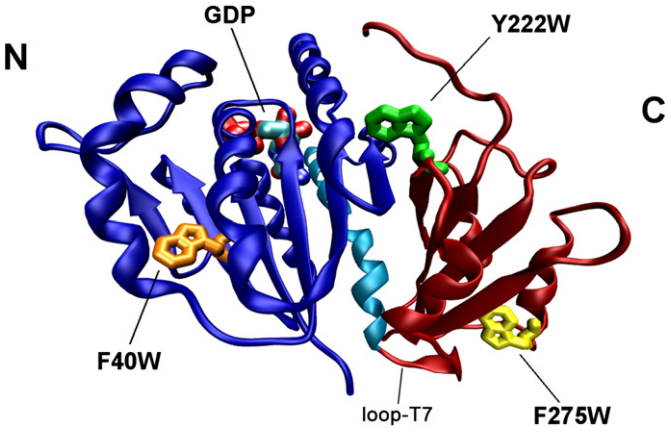

Fig. 1. FtsZ structure showing Trp introduced by mutagenesis. FtsZ structural model showing the position of the three tryptophans introduced by site-directed mutagenesis. The nucleotide binding domain (N) and the catalytic domain (C) were colored in blue and red, respectively. The H7 helix is considered the boundary between both domains and was colored in cyan. For simplicity, the three tryptophans introduced at positions 40 (orange), 222 (green) and 275 (yellow) are all shown in the same molecule. This figure was prepared using V.M.D. [36] and refined with POV-Ray version 3.6 (Persistence Of Vision Raytracer Pty, Ltd.).

2.3. Tryptophan steady-state fluorescence

Corrected emission spectra of total protein fluorescence were measured on an ISS PC1 spectrofluorimeter (ISS, Champaign, IL) using 275 nm (16 nm bandpass) as the excitation wavelength. For quenching experiments, emission spectra were recorded on a Perkin-Elmer LS-50 spectrofluorimeter (Perkin-Elmer, Waltham, MA) excited at 295 nm. Spectroscopic grade acrylamide (Merck, Germany) was added to protein mixtures in aliquots from a 1 M stock solution. Fluorescence intensities were corrected for dilution effects. The proteins stocks were dialyzed against 50 mM potassium phosphate buffer pH 6.5 before adjusting the concentration to the indicated values. The temperature was kept constant at 25 °C using a circulating water bath. All measurements were performed in 10 × 4 mm quartz cuvettes.

2.4. Tryptophan time-resolved fluorescence

Frequency domain time-resolved fluorescence was recorded using an ISS Chronos fluorometer. Samples were excited using a 300-nm LED in conjunction with a 295-nm band pass interference filter (Semrock, Rochester, NY), resulting in a nominal excitation maximum of 298-nm. Using a magic-angle polarizer configuration (vertical excitation polarization and 55° emission polarizer), the emission was collected through two 320-nm long pass filters to block scattered light. Proteins stocks were dialyzed against 50 mM potassium phosphate buffer pH 6.5. Then, the absorbance at the nominal excitation wavelength was adjusted to be just below 0.1 to avoid inner filter effects, resulting in protein concentration ~50 μM. N-acetyl-L-tryptophanamide (Sigma, St. Louis, MO) dissolved in pH 6.5 buffer was used as the reference lifetime, with an assigned 3.0 ns monoexponential decay. In the unfolding experiments, denaturant concentration was adjusted by adding aliquots from 6 M stock solutions. Measurements were performed in 10 × 4 mm quartz cuvettes at 25 °C. Fluorescence lifetimes were fit using GLOBALS for spectroscopy software (http:/www.lfd.uci.edu/globals/).

2.5. Phasor plots

The phasor method for representing time-resolved fluorescence has been reviewed elsewhere [21,23]. However, a brief description of the method is given here. The phasor approach offers a model-less method to visually assess aspects of excited state lifetimes. In particular, if the excited state decay is mono-exponential, the phasor point, for any light modulation frequency, will lie on the so-called “universal circle”, while the phasor points for multi-exponential decays will lie inside this circle (see Results). Complex decays may thus be displayed by a single point in phasor-space, which may be monitored to follow the effects of perturbations, such as structural transitions or the addition of denaturants, on the excited state properties. Experimental data used to build the phasor plots were obtained under the same conditions described above for ‘Tryptophan time-resolved fluorescence’. For further details on construction of phasor plots, see supporting information.

3. Results

3.1. In vitro activity and secondary structure of FtsZ wt and Trp mutants

We compared the homogeneity and oligomerization state of FtsZ wt and Trp mutant protein preparations using Coomassie blue-stained SDS-PAGE and analytical size-exclusion chromatography, respectively (Figure S1). For all proteins, densitometry analysis of the gel revealed a minimum 94% signal corresponding to the FtsZ band. Some differences were observed in the oligomerization state, varying within 92–97% monomer populations. Under these experimental conditions in the

Table 1
Biochemical parameters of FtsZ wt and the tryptophan mutants.

	Polymerization	GTPase activity		Corrected emission[c]	Acrylamide quenching[d]	
	$C_{C\text{-}pol}$ [a] μM	$C_{C\text{-}GTPase}$ [a] μM	Specific activity [b] μM Pi min^{-1} μM^{-1} FtsZ	λ_{max} nm	K_{SV} M^{-1}	k_q $\times 10^9$ M^{-1} s^{-1}
FtsZ wt	0.6 ± 0.4	0.2 ± 0.1	5.3 ± 0.2	ND	ND	ND
F40W	0.7 ± 0.4	0.4 ± 0.1	4.2 ± 0.4	330	3.1	1.2
Y222W	1.1 ± 0.3	0.2 ± 0.1	3.3 ± 0.2	340	6.0	1.0
F275W	1.2 ± 0.7	0.6 ± 0.1	4.4 ± 0.2	326	1.7	2.2

[a] C_C was obtained from intersection of linear regressions ($R^2 > 0.99$) with protein concentration axis. Uncertainties are 95% confidence intervals of linear regressions.
[b] Reported values are averages of specific activities calculated from samples at 3, 5 and 7 μM of protein concentration. Uncertainties are the standard deviations.
[c] ND, Not determined.
[d] Quenching constants were calculated using average lifetimes shown in Table 3.

absence of GTP and Mg^{+2}, we expected a majority of monomer species. Thus, the four protein preparations displayed similar purity and oligomerization state. A key aspect of FtsZ cooperative assembly is the existence of a critical concentration, C_C, which we determined from plots of the dependency of both polymerization and GTPase activity on protein concentration (Table 1 and Fig. 2). FtsZ wt and F40W displayed identical polymerization and GTPase kinetics, whereas Y222W and F275W mutants showed marked differences in both activities. The lower GTPase activity of Y222W is correlated with the extended time the mutant spent in the polymerized state compared to FtsZ wt. The F275W mutant showed a brief stationary polymerized state, but with comparable GTPase activity to FtsZ wt. The secondary structure contents of FtsZ wt and the Trp mutants were calculated from circular dichroism (CD) spectra (Figure S2). The fractions of alpha-helix, beta-strand and random coil, showed almost no differences between the four proteins. A small but significant difference was observed, however, in calculated fractions of helix and strand for F275W compared to FtsZ wt.

3.2. Steady state Trp fluorescence and acrylamide quenching

The corrected emission spectra of the Trp mutants are shown in Fig. 3. The emission maxima (λ_{max}) were obtained and it was noted that the bluer emission was from the F275W mutant, while the λ_{max} of Y222W was red-shifted relative to F40W mutant. In the three cases, the emission spectra are dominated by Trp fluorescence, independent of excitation wavelength, suggesting that tyrosine to tryptophan energy transfer could be taking place (since *E. coli* FtsZ has three tyrosine residues in its sequence). This transfer was confirmed by the excitation polarization spectra of the Trp mutants (Figure S3). Quenching of the intrinsic fluorescence by acrylamide was used to determine solvent accessibility of the Trp in FtsZ mutants (Stern–Volmer plots are shown in Fig. 3B). Calculated K_{SV} values, regarded as an indicator for solvent accessibility in single Trp proteins (Table 1), suggested that the most buried Trp was located at position 275, followed by the Trp at position 40 and the most solvent exposed at position 222 ($K_{SV\text{-}F275W} < K_{SV\text{-}F40W} < K_{SV\text{-}Y222W}$). This trend was also observed when analyzing the position

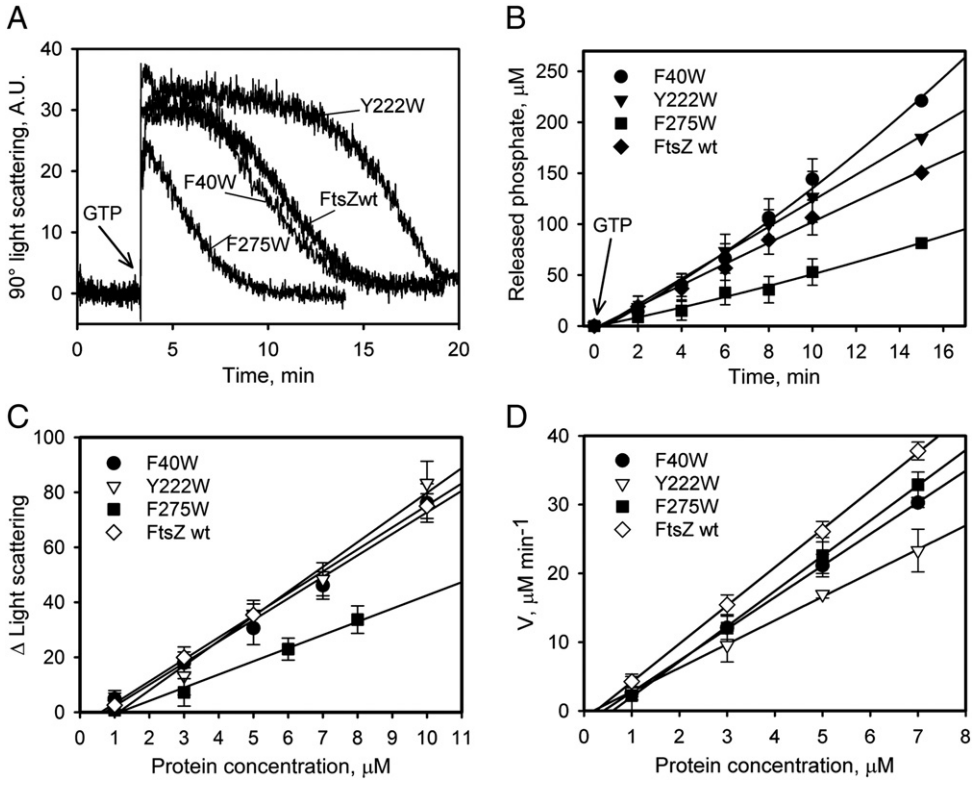

Fig. 2. In vitro functions of FtsZ wt and the Trp mutants. In vitro functions of FtsZ wt and the Trp mutants. Panel A, polymerization kinetics detected by 90° light scattering at 350 nm. Panel B, time-course of the GTP hydrolysis detected by release of inorganic phosphate. In panels A and B the protein concentrations used were 5 and 3 μM, respectively, and the solid lines were drawn to show data trends. Polymerization and GTPase activity were started by the addition of GTP (arrows). Panel C, protein concentration dependence of GTP-induced polymerization. Panel D, protein concentration dependence of the rates of GTP hydrolysis. The error bars in panels A and B are the standard deviations from duplicate and triplicate experiments, respectively.

of the emission maxima ($\lambda_{max\text{-}275} < \lambda_{max\text{-}40} < \lambda_{max\text{-}222}$), parameters also related to solvent accessibility due to the effect of solvent polarity on the emission. However, for collisional quenching, the accessibility parameter that best reflects efficiency of fluorophore quenching is the bimolecular quenching constant (k_q), defined as $K_{SV} = k_q \times \tau_0$, where τ_0 is the fluorescence lifetime in the absence of the quencher. The bimolecular quenching constants were calculated for Trp mutants using the averaged fluorescence lifetimes given in Table 3 (see below). These values indicated that tryptophan in position 275 was more efficiently quenched by acrylamide than the tryptophans in positions 40 and 222, which both exhibited lower, but similar, solvent accessibilities ($k_{q\ -222} \sim k_{q\ -40} < k_{q\ -275}$).

3.3. Tryptophan time-resolved fluorescence in the presence of GDP or GTP

Trp fluorescence was used to characterize the predicted conformational changes induced by exchange between GDP and GTP. To confirm that the proteins were bound to the nucleotides, we measured the apparent dissociation constants using the fluorescent analogues mant-GDP/GTP (Table 2). Anisotropy as a function of protein concentration indicated binding of the mant-nucleotides in all cases (Figure S4). The Trp mutants were incubated in the presence of 500 μM GDP and GTP, and based on the measured K_d we calculated average bound fractions of 0.93 ± 0.02 and 0.97 ± 0.01, respectively. Then, frequency domain time-resolved fluorescence data were measured (Figure S5). Fluorescence lifetimes, τ_i, and fractional intensities, f_i, were calculated from fits of experimental data using either a model of three discrete exponential decays or using a continuous distribution of lifetimes and one discrete component (Tables 3 and 4). To facilitate analysis of Trp time-resolved fluorescence, a graphical depiction of fit results is shown in Fig. 4. The averaged lifetimes were determined using the relationship $f_i \times \tau_i = \tau_{ave}$ and the observed values followed the same trend, F40W < F275W < Y222W, for both models, regardless of the nucleotide bound. F40W and F275W mutants did not show any significant change in their lifetime components, or fractional contributions, resulting in identical averaged lifetimes when incubated with GDP or GTP. In contrast, a reduction in all lifetime components was observed in the Y222W mutant, resulting in an overall ~1 ns decrease in the average fluorescence lifetime when comparing GDP- and GTP-bound states.

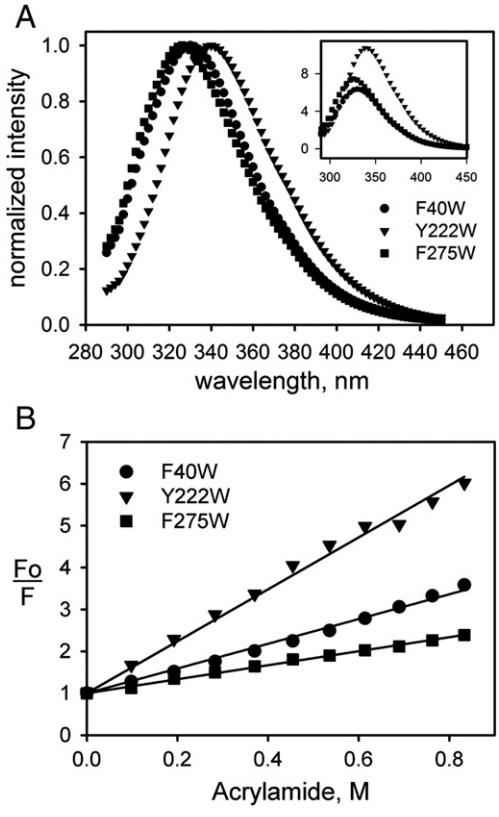

Fig. 3. Steady-state fluorescence measurements of FtsZ Trp mutants. Steady-state fluorescence measurements of FtsZ Trp mutants. Panel A, corrected emission spectra of tryptophan fluorescence at 25 μM protein concentration. The inset displays corrected spectra before normalization. Panel B, Stern–Volmer plots for collisional quenching at 10 μM protein concentration; the solid lines are the best fits of the experimental data using parameters reported in Table 1.

Table 2
Apparent dissociation constants for exchange of Mant nucleotides to FtsZ wt and the Trp mutants.

	Mant-GDP		Mant-GTP	
	K_d [a] $\times 10^{-6}$ M	$f_{b\text{-}500\ \mu M\ GDP}$	K_d $\times 10^{-6}$ M	$f_{b\text{-}500\ \mu M\ GTP}$
FtsZwt	28 ± 5	0.95	22 ± 4	0.96
F40W	25 ± 4	0.95	10 ± 2	0.98
Y222W	36 ± 6	0.93	16 ± 2	0.97
F275W	64 ± 13	0.89	20 ± 3	0.96
r_{free}	0.041 ± 0.003 [b]		0.054 ± 0.005	
r_{bound}	0.336 ± 0.035		0.322 ± 0.029	

[a] The uncertainties of calculated dissociation constants are the standard errors of the fits.
[b] Anisotropies of the free and bound states are the averages ± sd among all four proteins.

3.4. Conformational transitions of FtsZ mutants characterized by phasor plots.

Analysis of Trp lifetimes showed that FtsZ undergoes a local rearrangement between GDP- and GTP-bound states that lowers the Trp fluorescence lifetime at position 222 (see above). These results may be better compared using the model-less phasor plot. Thus, the phasor plots of FtsZ Trp mutants, bound to GDP or GTP, were constructed with the same data used to calculate fluorescence lifetimes (Fig. 5). The solid line is the so-called universal circle. Phasor points for single exponential lifetimes all lie on the universal circle. For example, the phasor plot for NATA (monoexponential fluorescence decay of 3 ns) shows that all phasor points are located on the universal circle (Fig. 5 A). The phasor points of the mutants F40W and F275W lie inside the universal circle, indicating lifetime heterogeneity. In contrast, the phasor points of Y222W mutant bound to GDP are very close to the universal circle suggesting near monoexponential intensity decay kinetics. When comparing the frequency dependent trend of the phasor points (moving counter-clockwise from low to high frequencies in

Table 3
Lifetime analysis using discrete components for the Trp mutants bound to GPD or GTP.

	τ_1 ns	τ_2 ns	τ_3 ns	f_1	f_2	f_3	τ_{ave} ns	χ^2
F40W-GDP	0.17 [a] ±0.01	1.49 ±0.01	5.88 ±0.52	0.05 ±0.04	0.68 ±0.01	0.26 ±0.01	2.6	1.4
F40W-GTP	0.18 ±0.11	1.42 ±0.04	5.91 ±0.22	0.06 ±0.01	0.67 ±0.01	0.28 ±0.01	2.6	0.7
Y222W-GDP	0.60 ±0.17	2.92 ±0.56	6.72 ±0.27	0.02 ±0.01	0.14 ±0.08	0.84 ±0.01	6.1	0.6
Y222W-GTP	0.05 ±0.13	1.95 ±0.26	6.32 ±0.19	0.02 ±0.06	0.28 ±0.03	0.70 ±0.01	5.0	0.9
F275W-GDP	0.23 ±0.05	1.74 ±0.15	5.78 ±0.19	0.08 ±0.01	0.37 ±0.02	0.54 ±0.01	3.8	0.7
F275W-GTP	0.21 ±0.05	1.68 ±0.14	5.83 ±0.17	0.09 ±0.02	0.36 ±0.02	0.55 ±0.01	3.8	0.9

[a] For data analysis, a constant standard error of 0.2° for the phase angle and 0.004 for modulation was used. Uncertainties are the standard errors of the fits.

Table 4
Lifetime analysis using a continuous Lorentzian distribution and one discrete component for the mutants bound to GDP or GTP.

	f_1	Center ns	Width ns	f_2	τ_2	χ^2
F40W-GDP	0.68 [b] ±0.01	2.6 ±0.1	2.4 ±0.2	0.32 ±0.02	1.1 ±0.2	1.2
F40W-GTP	0.65 ±0.01	2.5 ±0.1	2.3 ±0.2	0.35 ±0.1	1.0 ±0.1	1.5
Y222W-GDP	0.96 ±0.01	6.2 ±0.1	0.8 ±0.2	0.04 ±0.01	1.5 ±0.2	0.4
Y222W-GTP	0.91 ±0.03	5.0 ±0.5	2.3 ±0.2	0.09 ±0.02	1.2 ±0.2	1.7
F275W-GDP	0.88 ±0.01	3.3 ±0.1	3.0 ±0.1	0.12 ±0.01	0.6 ±0.1	1.3
F275W-GTP	0.90 ±0.05	3.4 ±0.1	3.1 ±0.1	0.10 ±0.01	0.5 ±0.1	1.6

[b] For data analysis, a constant standard error of 0.2° for the phase angle and 0.004 for modulation was used. Uncertainties are the standard errors of the fits.

Figs. 5 B–D), it was observed that F40W mutant experienced a small shift in the position of the phasor points to lower frequencies (clockwise), indicating a small but detectable decrease in lifetime components or fractional contributions. The Y222W mutant exhibited a greater shift in phasor positions, with points moving towards the center of the universal circle and slightly clockwise, to lower frequencies, therefore indicating a decrease in the average fluorescence lifetime. The F275W mutant did not show any shift in the positions of phasor points, at any frequencies, suggesting that the transition between GDP-bound to GTP-bound states does not perturb the environment near Trp 275.

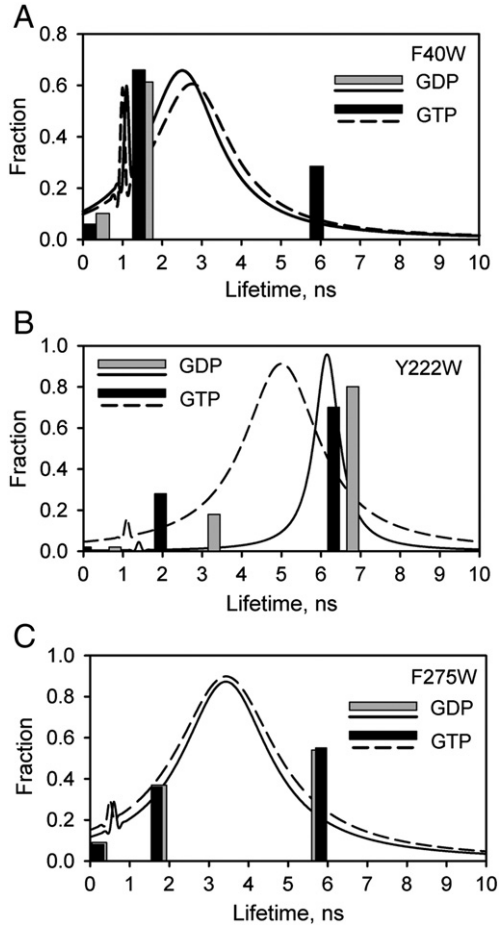

Fig. 4. Fluorescence lifetime analysis for FtsZ Trp mutants bound to GDP or GTP. Graphical depiction of fluorescence lifetime analysis for FtsZ Trp mutants bound to GDP or GTP. Panels A–C show an overlay between three discrete components analysis (vertical bars) and the continuous Lorentzian distribution analysis (lines). Lifetimes and fractional intensities used to fit the experimental data are reported in Tables 3 and 4.

Time-resolved fluorescence of Trp mutants was also exploited to analyze global conformational transitions, such as those found in protein unfolding. The chemical unfolding of the Trp mutants, at the same experimental conditions used to calculate fluorescence lifetimes, was induced by urea or GdmCl and the phasor points were calculated for each denaturant concentration. Fig. 6 A and B shows an expansion of phasor plot scales from the unfolding experiments measured at a frequency of 70 MHz, where the solid line on the left is the universal circle. At the beginning of the unfolding reaction (indicated by a star) the three mutants displayed specific positions in the two-dimensional phasor plane (G, S). The uniqueness in the position of phasor points under native conditions implies particular environment of the Trp in the protein structure. To facilitate a phenomenological analysis of unfolding using phasors, a three dimensional phasor plot was constructed for both denaturants (Fig. 6 C and D) by adding the coordinate of denaturant concentration [D] to data points (G, S, [D]). Then, a projection of phasor points as a function of denaturant concentration was drawn onto denaturant planes. In these plots, it is evident that at the beginning of the unfolding reaction (absence of denaturant), the phasor points of the three Trp are at different locations, while at the end of the reaction (~4 M denaturant) they are located close to each other. To compare the unfolding trajectories observed using phasors, with previous unfolding studies of FtsZ, two traces were drawn on denaturant planes of the 3D plots (dotted horizontal lines on Fig. 6 C and D). These lines indicate the two midpoints for the three-state unfolding of FtsZ calculated by the linear extrapolation method [15,16]. In case of urea-induced unfolding the phasor points for the three mutants tend to co-localize after the 2 M concentration midpoint, whereas in the case of GdmCl the same behavior was observed as early as 0.5 M concentration midpoint.

4. Discussion and conclusions

The FtsZ monomer in Fig. 1 was pictured according to the orientation of FtsZ protofilament proposed by Oliva et al. [24]. The Trp 40 is located at S2 strand in the hydrophobic core of the N domain and based on residue flexibility, the N domain has been ascribed as a rigid tertiary structural element [11,12]. However, due to its proximity to the nucleotide binding pocket, Trp 40 should report structural transitions related to the GTPase activity of FtsZ. The Trp in position 222 is located at the S7 strand in the surface of interaction between N and C domains, a moderately flexible structural element. Movements between N and C domains in FtsZ have been predicted based on molecular dynamics simulations [12,13]. In addition, Chen and Erickson [14] described a conformational transition upon polymerization that is consistent with a movement apart of the two domains. Moreover, a new crystal structure of FtsZ in complex with the cell-division inhibitor PC190723, regarded as the straight form of FtsZ, reveals a large conformational change involving the N and C domains [9,10]. Therefore, Trp 222 should report on conformational changes related to movements between N and C domains. Trp in position 275 is located in the flexible H10 helix, in close proximity to the bottom protofilament interface and facing the nucleotide binding pocket; therefore F275W mutant is a good construct to sense conformational changes between the GDP and GTP states. The Trp mutants were characterized to verify whether their polymerization and GTPase activities were comparable to FtsZ wt, specifically, the critical concentrations (C_C) were determined. Reported C_C values for polymerization vary between 0.5 and 2.5 μM, mainly due to different buffer conditions but also due to different purification procedures [2,11,22,25,26]. In this work, values for $C_{C\text{-pol}}$ of FtsZ wt and Trp mutants fall within the expected range. It was observed that values for C_C-GTPase were slightly lower than those for polymerization, indicating the GTP hydrolysis assay reported activity at protein concentrations in which the polymers were

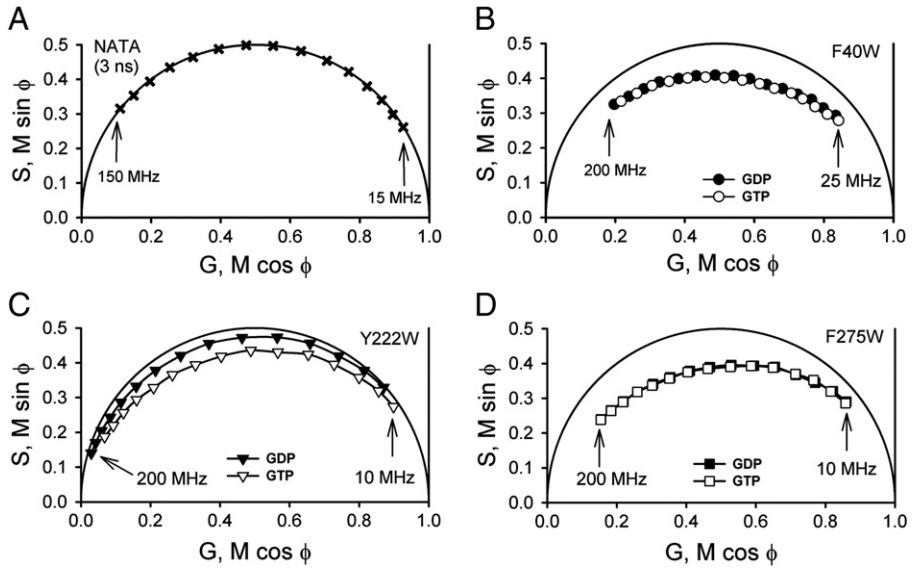

Fig. 5. Phasor plot analysis of FtsZ Trp mutants bound to GDP or GTP. Phasor plots of the time-resolved fluorescence of FtsZ Trp mutants bound to GDP or GTP. Panel A, phasor plot of NATA fluorescence for the range of modulation frequencies (symbols) used to measure its lifetime (15–150 MHz). Panels B–D, phasor plots of the tryptophan mutants in presence of GDP (closed symbols) and GTP (open symbols) for the range of frequencies used to measure their lifetimes (10–200 MHz). The solid line represents the universal circle on phasor plots.

too small to be detected in the light scattering experiment. Interestingly, the Y222W mutant displayed an extended stationary polymerization phase that is correlated to a 38% reduction in GTPase specific activity, resulting in a two-fold increase in $C_{C\text{-}pol}$ when compared to FtsZ wt. This observation suggests that the Y222W mutation imposes a structural constraint that retains the protein in the assembly competent form, therefore prolonging the stationary polymerized state. In contrast, a stationary phase was almost absent in the polymerization of the F275W mutant (which also showed a two-fold increase in $C_{C\text{-}pol}$), whereas the specific GTPase activity was reduced 25%. This observation suggested weaker longitudinal interactions of the F275W subunits within the filaments that could be linked to the α → β secondary structure transition detected by CD. Quantitative information about tryptophan solvent accessibility was obtained by acrylamide quenching experiments. The trend observed in the calculated K_{SV}, also observed in emission maxima, suggested that Trp at position 275 should be buried in the FtsZ structure, while Trp 222 should be solvent exposed. However, the true accessibility parameter is the bimolecular quenching constant, k_q, that takes into account the fluorescence lifetime of the fluorophore [27]. A comparison between calculated k_q to that of L-tryptophan in solution, $k_{q\text{-}Trp} = 6 \times 10^9\ M^{-1}\ s^{-1}$ [28], indicated that all Trp are buried from solvent accessibility. Specifically, Trp 40 and Trp 222 are highly buried and Trp 275 is slightly more solvent exposed. This conclusion would be exactly the opposite if we consider K_{SV} values and emission maxima, supporting

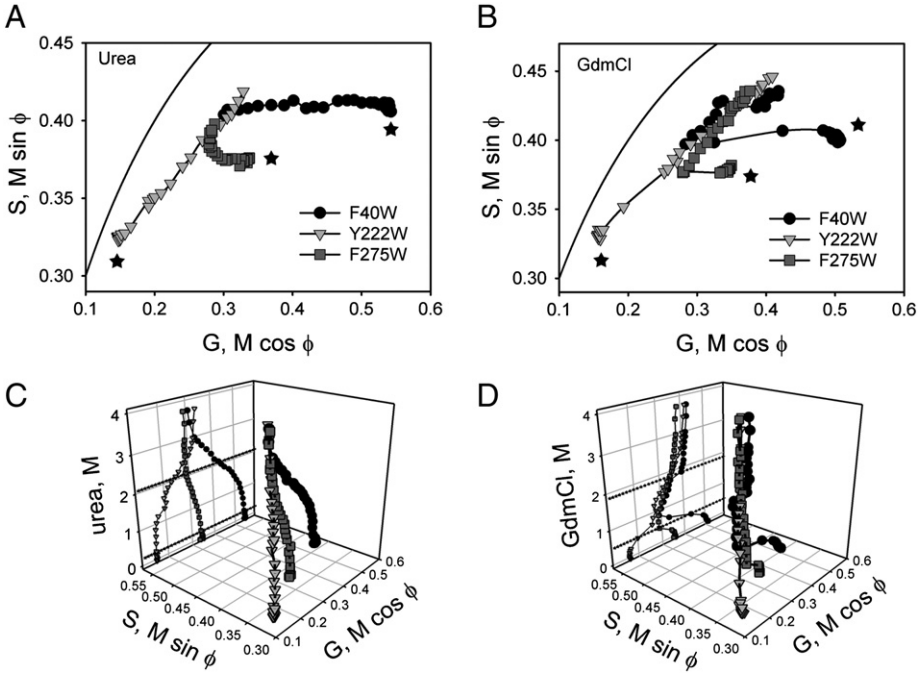

Fig. 6. Phasor plot analysis for chemical unfolding of FtsZ Trp mutants. Phasor plots of the chemical unfolding of FtsZ Trp mutants. The unfolding transition was monitored at a modulation frequency of 70 MHz. The calculated phasor points were plotted as a function of urea and GdmCl concentration (symbols). Panels A and B show an expanded view of the two-dimension phasor plots (G, S) of the unfolding reaction where the starting point was indicated by a star. The solid lines in 2D phasor plots indicate the universal circle. Panels C and D show an expanded view of the three-dimension phasor plots (G, S, [D]) including a denaturant concentration coordinate.

the fact that inferring tryptophan accessibility directly from spectral parameters could be misleading.

Tryptophan fluorescence was used to characterize the predicted conformational changes induced by exchange between GDP and GTP. Biochemical characterization indicated that the Trp mutants polymerize and hydrolyze GTP to an extent comparable to FtsZ wt. However, observed differences in the kinetics for Y222W and F275W mutants suggested that nucleotide binding could be impaired. We therefore quantified the apparent dissociation constants using fluorescent nucleotide analogues (Table 2) and found the proteins were at least 90% bound to the nucleotides. Binding of Mant-GDP/-GTP to apoFtsZ from *Methanococcus jannaschii* has been elegantly demonstrated using the increase in fluorescence anisotropy upon binding, resulting in K_d of 5.9×10^{-8} M and 5.6×10^{-8} M, respectively [29]. These values are two orders of magnitude below the K_d found in this work for *E. coli* FtsZ. We note that protein preparations used in this work contained stoichiometric amounts of nucleotide, as demonstrated by a spectrophotometric analysis (see supporting information); therefore we measured nucleotide exchange and expected lower affinities than reported for *M. jannaschii* apoFtsZ. Also, the oligomerization state of the protein is critical for the interpretation of tryptophan fluorescence lifetime as a reporter of FtsZ conformational changes. In this regard, we have previously shown that FtsZ-GDP weakly self-associates into dimers and tetramers [16]. In contrast, FtsZ-GTP polymerizes into short filaments, bundles or sheets depending on buffer conditions [2]. These results indicate that in our experimental conditions the observed changes in tryptophan fluorescence lifetime are coupled to any changes in the association state of the protein.

Time-resolved fluorescence data of Trp mutants was fit using either a sum of monoexponential decays or using the continuous Lorentzian distribution approach. These models imply that Trp exist in a finite set of conformations, for the first case, and in a distribution of isoenergetic conformations for the later model. For Trp in aqueous solution, the observed excited state decay depends upon the pH and a short (~0.5 ns) component has been attributed to a particular rotamer [30,31]. In single tryptophan containing proteins, multiexponential fluorescence decay is often attributed to ground state rotameric conformations that impose different environments on the indole group. In case of continuous distributions, ground state conformational heterogeneity translates into excited state heterogeneity, resulting in distributions of fluorescence lifetimes [32]. With both models the same conclusions were obtained, exchange of GDP by GTP did not change the fluorescence lifetime of F40W and F275W, whereas a significant decrease of ~1 ns was observed in the GTP-bound state for the Y222W mutant. Trp 40 is located in a rigid environment in the FtsZ structure; therefore large conformational changes were unexpected. In contrast, Trp 275 did not report conformational changes which was surprising since it is located in a flexible structural element and buried in the bottom protofilament interface. A plausible explanation for this behavior is the fast conformational transition after nucleotide hydrolysis, followed by rapid release of the GDP. This conclusion is supported by the short stationary polymerized phase observed, and by the lower affinity found for GDP nucleotide. In case of Y222W, a conformational change was expected since a movement between N and C domains was predicted computationally and demonstrated experimentally [9,10,12–14]. Interestingly, in the distribution analysis of Trp 222 in the presence of GDP, a narrower distribution of lifetimes was observed relative to that of GTP-bound state. The width of the lifetime distributions is related to the mobility of tryptophan residues in the protein structure, increasing as mobility decreases [17,31]. We can then surmise that Trp 222 has a reduced mobility in the GTP state, a conclusion that agrees with an increased rigidity at the domain interface due to the polymerized state of the protein.

We applied the modeless phasor plot to time-resolved fluorescence of the Trp mutants. In the phasor plot, a single exponential decay (homogeneous) will always fall on the universal circle whereas heterogeneous emissions place the phasor points inside the universal circle [33]. By comparing the phasor plots of Trp mutants for the GDP- and GTP-bound states, we observed similar behaviors to those discussed above. The Y222W mutant exhibited the largest conformational change, followed by a slight shift in phasor points for the F40W mutant, whereas the F275W mutant did not report changes in phasor points. We previously studied chemical unfolding of FtsZ using steady-state and time-resolved fluorescence and found that urea and GdmCl resulted in different unfolding pathways [11,16]. In the case of urea, the proposed mechanism of unfolding involves an expansion of the hydrophobic core followed by solvation of side chains by water and urea, therefore stabilizing non-native conformations [34]. Here, chemical unfolding of Trp mutants followed by phasors plots showed different pathways depending on denaturant and position of the Trp in the FtsZ structure. In the native state, i.e., without denaturant, the phasor points are located on different positions inside the universal circle indicating unique environments of the tryptophan. The increase in denaturant concentration induced a displacement of phasor points, for both denaturants, suggesting a change in the micro-environment surrounding the Trp. In the case of urea, we observed an almost complete co-localization of phasor points at >3 M urea and considering that total loss of secondary structure was detected at ~3 M urea, then the co-localization of phasor points represents the unfolded state of the protein. In the case of GdmCl, the transition from the native state phasor position to unfolded state phasor co-localization occurred as early as 1.5 M denaturant; hence we may conclude that GdmCl unfolds FtsZ more effectively than urea. The displacement of the phasor points after the second unfolding transition is due to binding of the denaturant to the polypeptide backbone. This behavior was also described in the classical linear extrapolation method as the linear dependency of the spectroscopic signal with increasing concentration of denaturant, and has been regarded as the post-unfolding transition [35].

Acknowledgments

The authors thank Felipe Villanelo for help on construction and analysis of the FtsZ structural model and Dr. Enrico Gratton for discussions on tryptophan lifetime data analysis. This work was supported by FP7 EC DIVINOCELL grant 223431 and Fondo Nacional de Desarrollo Científico y Tecnológico grant 1130711 (to O.M.). F.M.-F. received fellowships from Becas Chile and Programa de Mejoramiento de la Calidad y Equidad de la Educación, and was supported by Comisión Nacional de Investigación Científica y Tecnológica grant 24090139.

Appendix A. Supplementary data

Additional supporting information including Materials and Methods and Supplementary Figures S1–S5 can be found online in the file: FtsZ_TrpMutants_SupportingMaterial.pdf. doi: http://dx.doi.org/10.1016/j.bbapap.2014.03.012

References

[1] H.P. Erickson, D.E. Anderson, M. Osawa, FtsZ in bacterial cytokinesis: cytoskeleton and force generator all in one, Microbiol. Mol. Biol. Rev. 74 (2010) 504–528.
[2] A. Mukherjee, J. Lutkenhaus, Analysis of FtsZ assembly by light scattering and determination of the role of divalent metal cations, J. Bacteriol. 181 (1999) 823–832.
[3] A. Mukherjee, J. Lutkenhaus, Dynamic assembly of FtsZ regulated by GTP hydrolysis, EMBO J. 17 (1998) 462–469.
[4] C. Lu, M. Reedy, H.P. Erickson, Straight and curved conformations of FtsZ are regulated by GTP hydrolysis, J. Bacteriol. 182 (2000) 164–170.
[5] S. Huecas, J.M. Andreu, Polymerization of nucleotide-free, GDP- and GTP-bound cell division protein FtsZ: GDP makes the difference, FEBS Lett. 569 (2004) 43–48.
[6] J. Löwe, L. Amos, Crystal structure of the bacterial cell-division protein FtsZ, Nature 391 (1998) 203–206.
[7] M.A. Oliva, D. Trambaiolo, J. Lowe, Structural insights into the conformational variability of FtsZ, J. Mol. Biol. 373 (2007) 1229–1242.
[8] H. Erickson, Modeling the physics of FtsZ assembly and force generation, PNAS 106 (2009) 9238–9243.

[9] T. Matsui, J. Yamane, N. Mogi, H. Yamaguchi, H. Takemoto, M. Yao, I. Tanaka, Structural reorganization of the bacterial cell-division protein FtsZ from *Staphylococcus aureus*, Acta Crystallogr. D Biol. Crystallogr. 68 (2012) 1175–1188.
[10] N.L. Elsen, J. Lu, G. Parthasarathy, J.C. Reid, S. Sharma, S.M. Soisson, K.J. Lumb, Mechanism of action of the cell-division inhibitor PC190723: modulation of FtsZ assembly cooperativity, J. Am. Chem. Soc. 134 (2012) 12342–12345.
[11] R. Díaz-Espinoza, A.P. Garcés, J.J. Arbildua, F. Montecinos, J.E. Brunet, R. Lagos, O. Monasterio, Domain folding and flexibility of *Escherichia coli* FtsZ determined by tryptophan site-directed mutagenesis, Protein Sci. 16 (2007) 1543–1556.
[12] A.J. Martín-Galiano, R.M. Buey, M. Cabezas, J.M. Andreu, Mapping flexibility and the assembly switch of cell division protein FtsZ by computational and mutational approaches, J. Biol. Chem. 285 (2010) 22554–22565.
[13] K. Natarajan, S. Senapati, Probing the conformational flexibility of monomeric FtsZ in GTP-bound, GDP-bound, and nucleotide-free states, Biochemistry 52 (2013) 3543–3551.
[14] Y. Chen, H.P. Erickson, Conformational changes of FtsZ reported by tryptophan mutants, Biochemistry 50 (2011) 4675–4684.
[15] J.M. Andreu, M.A. Oliva, O. Monasterio, Reversible unfolding of FtsZ cell division proteins from archaea and bacteria. Comparison with eukaryotic tubulin folding and assembly, J. Biol. Chem. 277 (2002) 43262–43270.
[16] F. Montecinos-Franjola, J.A. Ross, S.A. Sanchez, J.E. Brunet, R. Lagos, D.M. Jameson, O. Monasterio, Studies on the dissociation and urea-induced unfolding of FtsZ support the dimer nucleus polymerization mechanism, Biophys. J. 102 (2012) 2176–2185.
[17] D.M. Jameson, E. Gratton, J.F. Eccleston, Intrinsic fluorescence of elongation factor Tu in its complexes with GDP and elongation factor Ts, Biochemistry 26 (1987) 3894–3901.
[18] S.A. Sánchez, J.E. Brunet, D.M. Jameson, R. Lagos, O. Monasterio, Tubulin equilibrium unfolding followed by time-resolved fluorescence and fluorescence correlation spectroscopy, Protein Sci. 13 (2004) 81–88.
[19] N.G. James, J.A. Ross, A.B. Mason, D.M. Jameson, Excited-state lifetime studies of the three tryptophan residues in the N-lobe of human serum transferrin, Protein Sci. 19 (2010) 99–110.
[20] N.G. James, J.A. Ross, M. Stefl, D.M. Jameson, Applications of phasor plots to in vitro protein studies, Anal. Biochem. 410 (2011) 70–76.
[21] D.M. Jameson, C.M. Vetromile, N.G. James, Investigations of protein–protein interactions using time-resolved fluorescence and phasors, Methods 59 (2013) 278–286.
[22] E. Nova, F. Montecinos, J.E. Brunet, R. Lagos, O. Monasterio, 4′,6-Diamidino-2-phenylindole (DAPI) induces bundling of *Escherichia coli* FtsZ polymers inhibiting the GTPase activity, Arch. Biochem. Biophys. 465 (2007) 315–319.
[23] M. Stefl, N.G. James, J.A. Ross, D.M. Jameson, Applications of phasors to in vitro time-resolved fluorescence measurements, Anal. Biochem. 410 (2011) 62–69.
[24] M.A. Oliva, S.C. Cordell, J. Lowe, Structural insights into FtsZ protofilament formation, Nat. Struct. Mol. Biol. 11 (2004) 1243–1250.
[25] E.L. White, L.J. Ross, R.C. Reynolds, L.E. Seitz, G.D. Moore, D.W. Borhani, Slow polymerization of *Mycobacterium tuberculosis* FtsZ, J. Bacteriol. 182 (2000) 4028–4034.
[26] J.M. Gonzalez, M. Jimenez, M. Velez, J. Mingorance, J.M. Andreu, M. Vicente, G. Rivas, Essential cell division protein FtsZ assembles into one monomer-thick ribbons under conditions resembling the crowded intracellular environment, J. Biol. Chem. 278 (2003) 37664–37671.
[27] M.R. Eftink, C.A. Ghiron, Dynamics of a protein matrix revealed by fluorescence quenching, Proc. Natl. Acad. Sci. U. S. A. 72 (1975) 3290–3294.
[28] J.R. Lakowicz, Principles of Fluorescence Spectroscopy, Third edition Springer Baltimore, MA, 2006.
[29] S. Huecas, C. Schaffner-Barbero, W. Garcia, H. Yebenes, J.M. Palacios, J.F. Diaz, M. Menendez, J.M. Andreu, The interactions of cell division protein FtsZ with guanine nucleotides, J. Biol. Chem. 282 (2007) 37515–37528.
[30] J.M. Beechem, L. Brand, Time-resolved fluorescence of proteins, Annu. Rev. Biochem. 54 (1985) 43–71.
[31] J.A. Ross, D.M. Jameson, Time-resolved methods in biophysics. 8. Frequency domain fluorometry: applications to intrinsic protein fluorescence, Photochem. Photobiol. Sci. 7 (2008) 1301–1312.
[32] J.R. Alcala, E. Gratton, F.G. Prendergast, Interpretation of fluorescence decays in proteins using continuous lifetime distributions, Biophys. J. 51 (1987) 925–936.
[33] G.I. Redford, R.M. Clegg, Polar plot representation for frequency-domain analysis of fluorescence lifetimes, J. Fluoresc. 15 (2005) 805–815.
[34] B.J. Bennion, V. Daggett, The molecular basis for the chemical denaturation of proteins by urea, PNAS 100 (2003) 5142–5147.
[35] D.W. Bolen, M.M. Santoro, Unfolding free energy changes determined by the linear extrapolation method. 2. Incorporation of delta G degrees N-U values in a thermodynamic cycle, Biochemistry 27 (1988) 8069–8074.
[36] W. Humphrey, A. Dalke, K. Schulten, VMD: visual molecular dynamics, J. Mol. Graph. 14 (1996) 33–38 (27–38)